Diffusion and Reactions in Fractals and Disordered Systems

Daniel ben-Avraham
Clarkson University
and
Shlomo Havlin
Bar-Ilan University

CAMBRIDGE
UNIVERSITY PRESS

PUBLISHED BY THE PRESS SYNDICATE OF THE UNIVERSITY OF CAMBRIDGE
The Pitt Building, Trumpington Street, Cambridge, United Kingdom

CAMBRIDGE UNIVERSITY PRESS
The Edinburgh Building, Cambridge CB2 2RU, UK
40 West 20th Street, New York, NY 10011-4211, USA
10 Stamford Road, Oakleigh, VIC 3166, Australia
Ruiz de Alarcón 13, 28014, Madrid, Spain
Dock House, The Waterfront, Cape Town 8001, South Africa

http://www.cambridge.org

© Daniel ben-Avraham and Shlomo Havlin 2000

This book is in copyright. Subject to statutory exception
and to the provisions of relevant collective licensing agreements,
no reproduction of any part may take place without
the written permission of Cambridge University Press.

First published 2000

Printed in the United Kingdom at the University Press, Cambridge

Typeface Times 11/14pt. *System* LaTeX 2_ε [DBD]

A catalogue record of this book is available from the British Library

Library of Congress Cataloguing in Publication data

Ben-Avraham, Daniel, 1957–
Diffusion and reactions in fractals and disordered systems /
Daniel ben-Avraham and Shlomo Havlin.
p. cm. ISBN 0 521 62278 6 (hc.)
1. Diffusion. 2. Fractals. 3. Stochastic processes. I. Havlin, Shlomo. II. Title.
QC185.B46 2000
530.4′75–dc21 00-023591 CIP

ISBN 0 521 62278 6 hardback

Contents

Preface *page* xiii

Part one: Basic concepts 1

1 Fractals 3
1.1 Deterministic fractals 3
1.2 Properties of fractals 6
1.3 Random fractals 7
1.4 Self-affine fractals 9
1.5 Exercises 11
1.6 Open challenges 12
1.7 Further reading 12

2 Percolation 13
2.1 The percolation transition 13
2.2 The fractal dimension of percolation 18
2.3 Structural properties 21
2.4 Percolation on the Cayley tree and scaling 25
2.5 Exercises 28
2.6 Open challenges 30
2.7 Further reading 31

3 Random walks and diffusion 33
3.1 The simple random walk 33
3.2 Probability densities and the method of characteristic functions 35
3.3 The continuum limit: diffusion 37
3.4 Einstein’s relation for diffusion and conductivity 39
3.5 Continuous-time random walks 41
3.6 Exercises 43

3.7 Open challenges 44
3.8 Further reading 45

4 Beyond random walks 46
4.1 Random walks as fractal objects 46
4.2 Anomalous continuous-time random walks 47
4.3 Lévy flights and Lévy walks 48
4.4 Long-range correlated walks 50
4.5 One-dimensional walks and landscapes 53
4.6 Exercises 55
4.7 Open challenges 55
4.8 Further reading 56

Part two: Anomalous diffusion 57

5 Diffusion in the Sierpinski gasket 59
5.1 Anomalous diffusion 59
5.2 The first-passage time 61
5.3 Conductivity and the Einstein relation 63
5.4 The density of states: fractons and the spectral dimension 65
5.5 Probability densities 67
5.6 Exercises 70
5.7 Open challenges 71
5.8 Further reading 72

6 Diffusion in percolation clusters 74
6.1 The analogy with diffusion in fractals 74
6.2 Two ensembles 75
6.3 Scaling analysis 77
6.4 The Alexander–Orbach conjecture 79
6.5 Fractons 82
6.6 The chemical distance metric 83
6.7 Diffusion probability densities 87
6.8 Conductivity and multifractals 89
6.9 Numerical values of dynamical critical exponents 92
6.10 Dynamical exponents in continuum percolation 92
6.11 Exercises 94
6.12 Open challenges 95
6.13 Further reading 96

7 Diffusion in loopless structures 98
7.1 Loopless fractals 98

7.2 The relation between transport and structural exponents 101
7.3 Diffusion in lattice animals 103
7.4 Diffusion in DLAs 104
7.5 Diffusion in combs with infinitely long teeth 106
7.6 Diffusion in combs with varying teeth lengths 108
7.7 Exercises 110
7.8 Open challenges 112
7.9 Further reading 113

8 Disordered transition rates 114
8.1 Types of disorder 114
8.2 The power-law distribution of transition rates 117
8.3 The power-law distribution of potential barriers and wells 118
8.4 Barriers and wells in strips ($n \times \infty$) and in $d \geq 2$ 119
8.5 Barriers and wells in fractals 121
8.6 Random transition rates in one dimension 122
8.7 Exercises 124
8.8 Open challenges 125
8.9 Further reading 126

9 Biased anomalous diffusion 127
9.1 Delay in a tooth under bias 128
9.2 Combs with exponential distributions of teeth lengths 129
9.3 Combs with power-law distributions of teeth lengths 131
9.4 Topological bias in percolation clusters 132
9.5 Cartesian bias in percolation clusters 133
9.6 Bias along the backbone 135
9.7 Time-dependent bias 136
9.8 Exercises 138
9.9 Open challenges 139
9.10 Further reading 140

10 Excluded-volume interactions 141
10.1 Tracer diffusion 141
10.2 Tracer diffusion in fractals 143
10.3 Self-avoiding walks 144
10.4 Flory’s theory 146
10.5 SAWs in fractals 148
10.6 Exercises 151
10.7 Open challenges 152
10.8 Further reading 153

Part three: Diffusion-limited reactions 155

11 Classical models of reactions 157
11.1 The limiting behavior of reaction processes 157
11.2 Classical rate equations 159
11.3 Kinetic phase transitions 161
11.4 Reaction–diffusion equations 163
11.5 Exercises 164
11.6 Open challenges 166
11.7 Further reading 166

12 Trapping 167
12.1 Smoluchowski's model and the trapping problem 167
12.2 Long-time survival probabilities 168
12.3 The distance to the nearest surviving particle 171
12.4 Mobile traps 174
12.5 Imperfect traps 174
12.6 Exercises 175
12.7 Open challenges 176
12.8 Further reading 177

13 Simple reaction models 179
13.1 One-species reactions: scaling and effective rate equations 179
13.2 Two-species annihilation: segregation 182
13.3 Discrete fluctuations 185
13.4 Other models 187
13.5 Exercises 189
13.6 Open challenges 189
13.7 Further reading 190

14 Reaction–diffusion fronts 192
14.1 The mean-field description 192
14.2 The shape of the reaction front in the mean-field approach 194
14.3 Studies of the front in one dimension 195
14.4 Reaction rates in percolation 196
14.5 $A + B_{\mathrm{static}} \to C$ with a localized source of A particles 200
14.6 Exercises 201
14.7 Open challenges 202
14.8 Further reading 203

Part four: Diffusion-limited coalescence: an exactly solvable model 205

15 Coalescence and the IPDF method 207
15.1 The one-species coalescence model 207
15.2 The IPDF method 208
15.3 The continuum limit 211
15.4 Exact evolution equations 212
15.5 The general solution 213
15.6 Exercises 215
15.7 Open challenges 216
15.8 Further reading 216

16 Irreversible coalescence 217
16.1 Simple coalescence, $A + A \to A$ 217
16.2 Coalescence with input 222
16.3 Rate equations 223
16.4 Exercises 227
16.5 Open challenges 228
16.6 Further reading 228

17 Reversible coalescence 229
17.1 The equilibrium steady state 229
17.2 The approach to equilibrium: a dynamical phase transition 231
17.3 Rate equations 233
17.4 Finite-size effects 234
17.5 Exercises 236
17.6 Open challenges 237
17.7 Further reading 237

18 Complete representations of coalescence 238
18.1 Inhomogeneous initial conditions 238
18.2 Fisher waves 240
18.3 Multiple-point correlation functions 243
18.4 Shielding 245
18.5 Exercises 247
18.6 Open challenges 247
18.7 Further reading 248

19 Finite reaction rates 249
19.1 A model for finite coalescence rates 249
19.2 The approximation method 250
19.3 Kinetics crossover 251
19.4 Finite-rate coalescence with input 254

19.5 Exercises 256
19.6 Open challenges 257
19.7 Further reading 257

Appendix A The fractal dimension 258
Appendix B The number of distinct sites visited by random walks 260
Appendix C Exact enumeration 263
Appendix D Long-range correlations 266

References 272
Index 313

2

Percolation

Random fractals in Nature arise for a variety of reasons (dynamic chaotic processes, self-organized criticality, etc.) that are the focus of much current research. Percolation is one such chief mechanism. The importance of percolation lies in the fact that it models critical phase transitions of rich physical content, yet it may be formulated and understood in terms of very simple geometrical concepts. It is also an extremely versatile model, with applications to such diverse problems as supercooled water, galactic structures, fragmentation, porous materials, and earthquakes.

2.1 The percolation transition

Consider a square lattice on which each bond is present with probability p, or absent with probability $1-p$. When p is small there is a dilute population of bonds, and clusters of small numbers of connected bonds predominate. As p increases, the size of the clusters also increases. Eventually, for p large enough there emerges a cluster that spans the lattice from edge to edge (Fig. 2.1). If the lattice is infinite, the inception of the spanning cluster occurs sharply upon crossing a *critical threshold* of the bond concentration, $p = p_\mathrm{c}$.

The probability that a given bond belongs to the incipient infinite cluster, P_∞, undergoes a phase transition: it is zero for $p < p_\mathrm{c}$, and increases continuously as p is made larger than the critical threshold p_c (Fig. 2.2). Above and close to the transition point, P_∞ follows a power law:

$$P_\infty \sim (p - p_\mathrm{c})^\beta . \tag{2.1}$$

This phenomenon is known as the *percolation* transition. The name comes from the possible interpretation of bonds as channels open to the flow of a fluid in a porous medium (absent bonds represent blocked channels). At the transition point the fluid can percolate through the medium for the first time. The flow rate undergoes

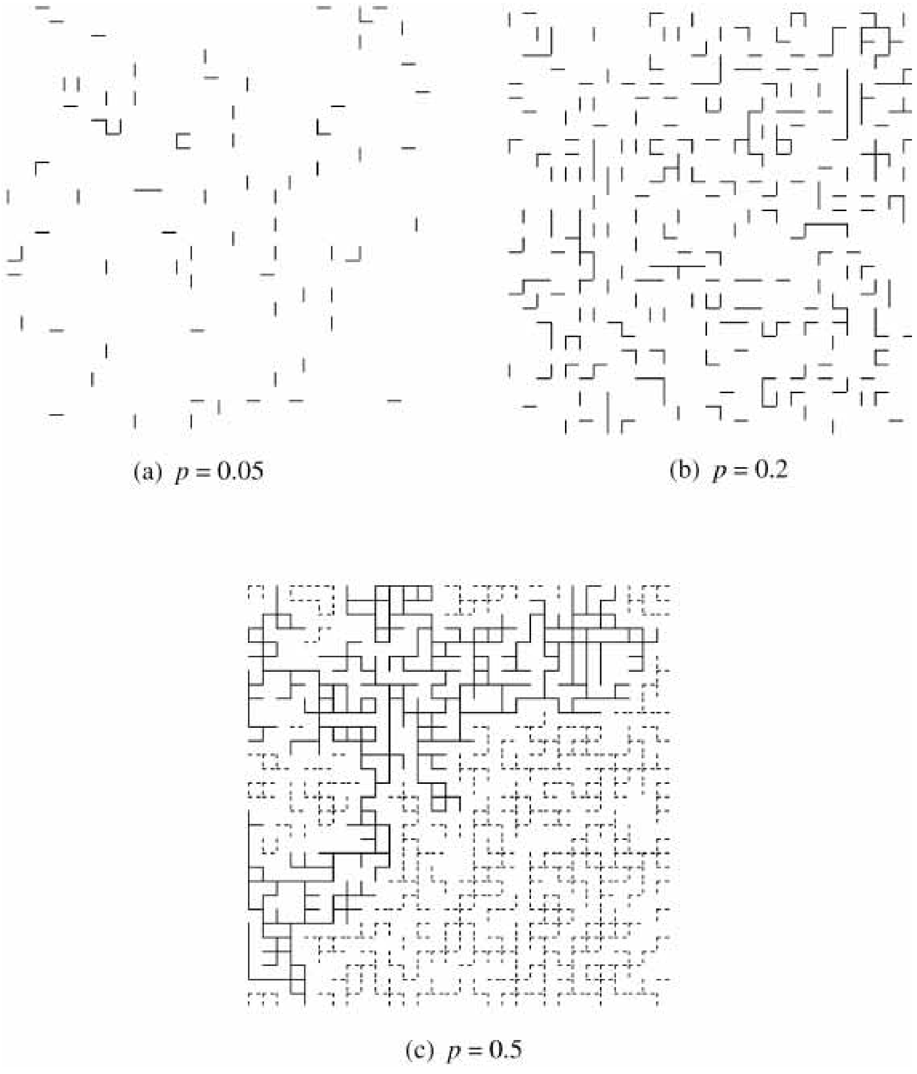

(a) $p = 0.05$

(b) $p = 0.2$

(c) $p = 0.5$

Fig. 2.1. Bond percolation on the square lattice. Shown are 40×40 square lattices, where bonds are present with probabilities $p = 0.05$ (a), 0.20 (b), and 0.50 (c). Notice how the clusters of connected bonds (i.e., the percolation clusters) grow in size as p increases. In (c) the concentration is equal to the critical concentration for bond percolation on the square lattice, $p_c = 0.5$. A cluster spanning the lattice (from top to bottom) appears for the first time. The bonds of this incipient infinite cluster are highlighted in bold.

a phase transition similar to that of P_∞. In fact, the transition is similar to all other continuous (second-order) phase transitions in physical systems. P_∞ plays the role of an *order parameter*, analogous to magnetization in a ferromagnet, and β is the *critical exponent* of the order parameter.

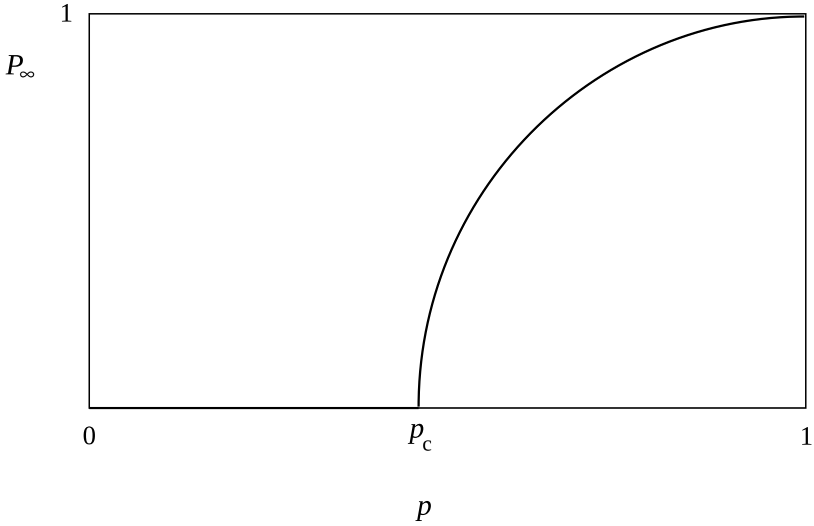

Fig. 2.2. A schematic representation of the percolation transition. The probability P_∞ that a bond belongs to the spanning cluster undergoes a sharp transition (in the thermodynamic limit of infinitely large systems): below a critical probability threshold p_c there is no spanning cluster, so $P_\infty = 0$, but P_∞ becomes finite when $p > p_c$.

There exists a large variety of percolation models. For example, the model above can be defined on a triangular lattice, or any other lattice besides the square lattice. In *site percolation* the percolating elements are lattice sites, rather than bonds. In that case we think of nearest-neighbor sites as belonging to the same cluster (Fig. 2.3). Other connectivity rules may be employed: in *bootstrap percolation* a subset of the cluster is connected if it is attached by at least two sites, or bonds. *Continuum percolation* is defined without resorting to a lattice – consider for example a set of circles randomly placed on a plane, where contact is made through their partial overlap (Fig. 2.4). Finally, one may consider percolation in different space dimensions. The percolation threshold p_c is affected by these various choices (Table 2.1), but critical exponents, such as β, depend only upon the space dimension. This insensitivity to all other details is termed *universality*. Clearly, critical exponents capture something very essential of the nature of the model at hand. They are used to classify critical phase transitions into *universality classes*.

Let us define some more of these important critical exponents. The typical length of finite clusters is characterized by the *correlation length* ξ. It diverges as p approaches p_c as

$$\xi \sim |p - p_c|^{-\nu}, \tag{2.2}$$

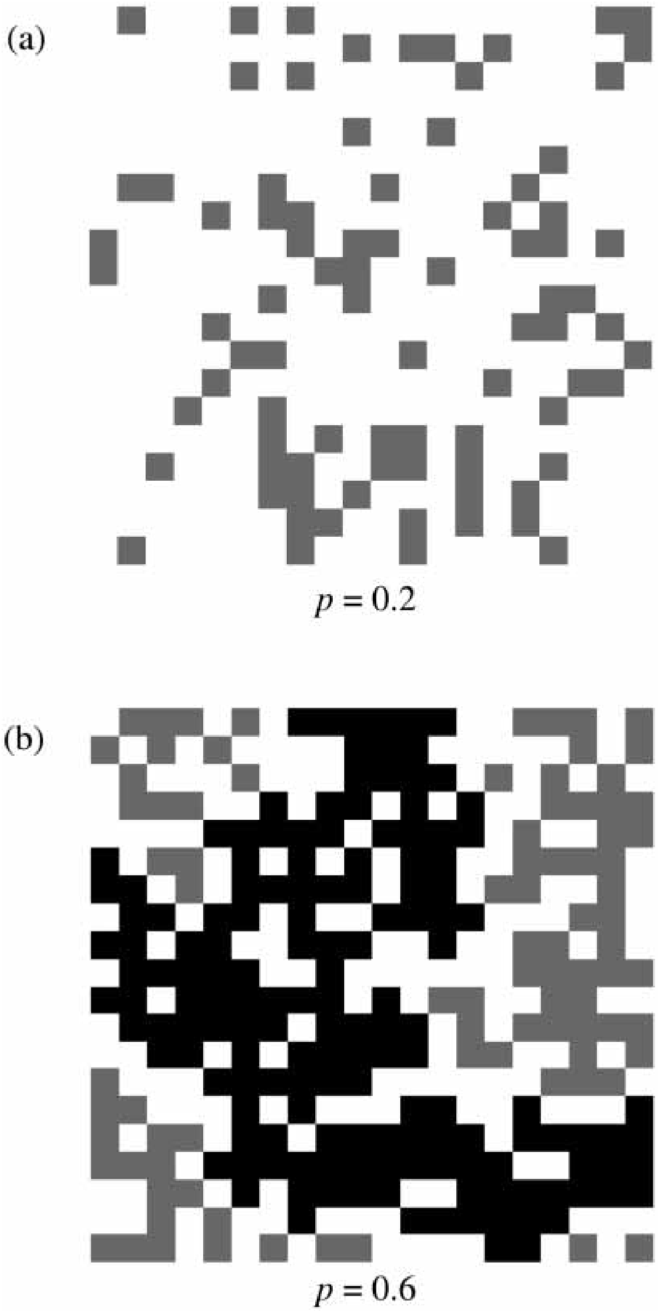

Fig. 2.3. Site percolation on the square lattice. Shown are 20×20 square lattices with sites occupied (gray squares) with probabilities $p = 0.2$ (a) and 0.6 (b). Nearest-neighbor sites (squares that share an edge) belong to the same cluster. The concentration in (b) is slightly above p_c of the infinite system, hence a spanning cluster results. The sites of the “infinite” cluster are in black.

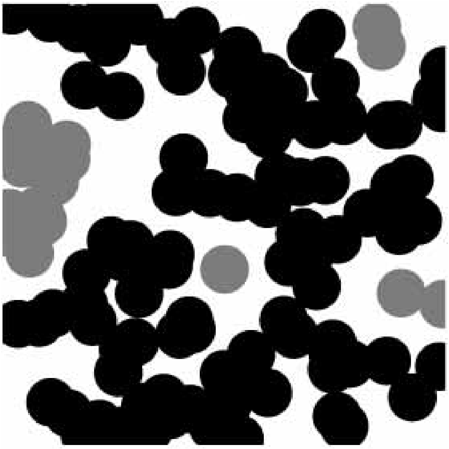

Fig. 2.4. Continuum percolation of circles on the plane. In this example the percolating elements are circles of a given diameter, which are placed *randomly* on the plane. Overlapping circles belong to the same cluster. As the concentration of circles increases the clusters grow in size, until a spanning percolating cluster appears (black circles). This type of percolation model requires no underlying lattice.

Table 2.1. *Percolation thresholds for several two- and three-dimensional lattices and the Cayley tree.*

Lattice	Percolation	
	Sites	Bonds
Triangular	$\frac{1}{2}$[a]	$2\sin(\pi/18)$[a]
Square	0.592 746 0[b,c]	$\frac{1}{2}$[a]
Honeycomb	0.697 043[d]	$1 - 2\sin(\pi/18)$[a]
Face-centered cubic	0.198[e]	0.120 163 5[c]
Body-centered cubic	0.254[e]	0.180 287 5[c]
Simple cubic (first nearest neighbor)	0.311 605[f,g]	0.248 812 6[c,h]
Simple cubic (second nearest neighbor)	0.137[i]	–
Simple cubic (third nearest neighbor)	0.097[i]	–
Cayley tree	$1/(z-1)$	$1/(z-1)$
Continuum percolation $d = 2$ (overlapping circles)	0.312 ± 0.005[j]	–
Continuum percolation $d = 3$ (overlapping spheres)	0.2895 ± 0.0005[k]	–

[a] Exact: Essam *et al.* (1978), Kesten (1982), Ziff (1992); [b] Ziff and Sapoval (1987); [c] Lorenz and Ziff (1998); [d] Suding and Ziff (1999); [e] Stauffer (1985a); [f] Strenski *et al.* (1991); [g] Acharyya and Stauffer (1998); [h] Grassberger (1992a); [i] Domb (1966); [j] Vicsek and Kertesz (1981), Kertesz (1981); and [k] Rintoul and Torquato (1997).

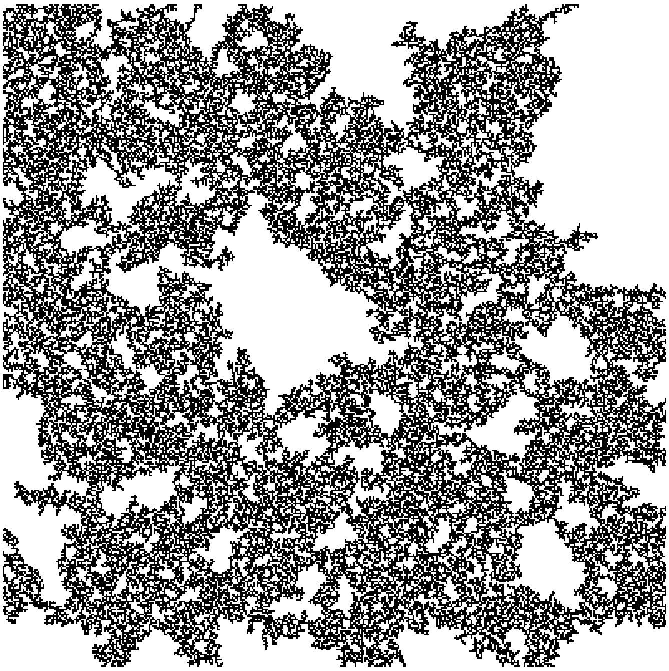

Fig. 2.5. An incipient infinite cluster. Shown is the spanning cluster in site percolation on the square lattice, as obtained from a computer simulation in a 400 × 400 square, with $p = 0.6$ (just above the percolation threshold). For clarity, occupied sites that do not belong to the spanning cluster have been removed, thus highlighting the presence of holes on all length scales – a characteristic feature of random fractals.

with the same critical exponent ν below and above the transition. The average mass (the number of sites in site percolation, or the number of bonds in bond percolation) of finite clusters, S, is analogous to the magnetic susceptibility in ferromagnetic phase transitions. It diverges about p_c as

$$S \sim |p - p_c|^{-\gamma}, \tag{2.3}$$

again with the same exponent γ on both sides of the transition. In the following sections we shall meet some more exponents and we shall see how they are related to each other.

2.2 The fractal dimension of percolation

The structure of percolation clusters can be well described by fractal concepts. Consider first the incipient infinite cluster at the critical threshold. An example is shown in Fig. 2.5. As is evident, the cluster contains holes on all length scales,

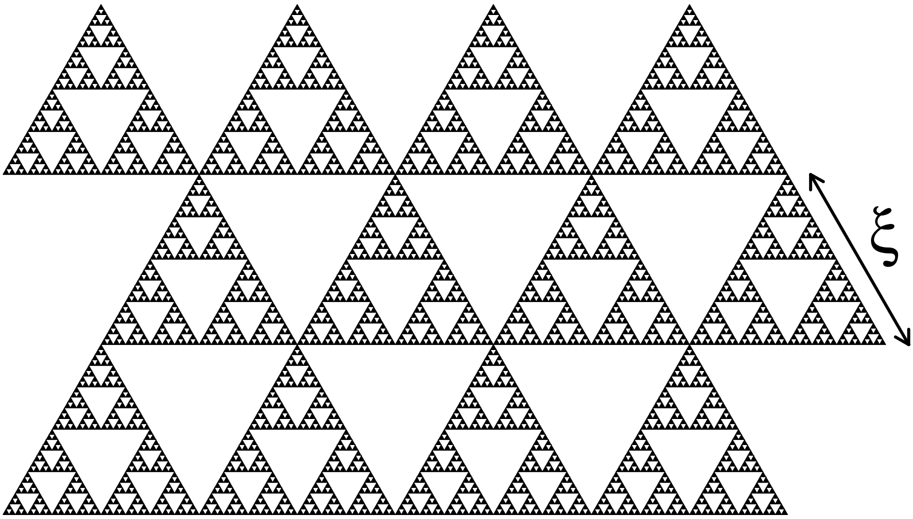

Fig. 2.6. A schematic representation of the infinite percolation cluster above p_c. The fractal features of the infinite cluster above the percolation threshold are represented schematically by repeating Sierpinski gaskets of length ξ, the so-called correlation length. There is self-similarity only at distances shorter than ξ, whereas on larger length scales the cluster is homogeneous (like a regular triangular lattice, in this drawing).

similar to the random Sierpinski carpet of Fig. 1.4b. In fact, with help of the box-counting algorithm, or other techniques from Chapter 1, one can show that the cluster is self-similar on all length scales (larger than the lattice spacing and smaller than its overall size) and can be regarded as a fractal. Its fractal dimension d_f describes how the mass S within a sphere of radius r scales with r:

$$S(r) \sim r^{d_f}. \tag{2.4}$$

$S(r)$ is obtained by averaging over many cluster realizations (in different percolation simulations), or, equivalently, averaging over different positions of the center of the sphere in a single infinite cluster.

Let us now examine percolation clusters off criticality. Below the percolation threshold the typical size of clusters is finite, of the order of the correlation length ξ. Therefore, clusters below criticality can be self-similar only up to the length scale of ξ. The system possesses a natural upper cutoff. Above criticality, ξ is a measure of the size of the *finite* clusters in the system. The incipient infinite cluster remains infinite in extent, but its largest holes are also typically of size ξ. It follows that the infinite cluster can be self-similar only up to length scale ξ. At distances larger than ξ self-similarity is lost and the infinite cluster becomes homogeneous. In other words, for length scales shorter than ξ the system is *scale invariant* (or self-similar) whereas for length scales larger than ξ the system is *translationally*

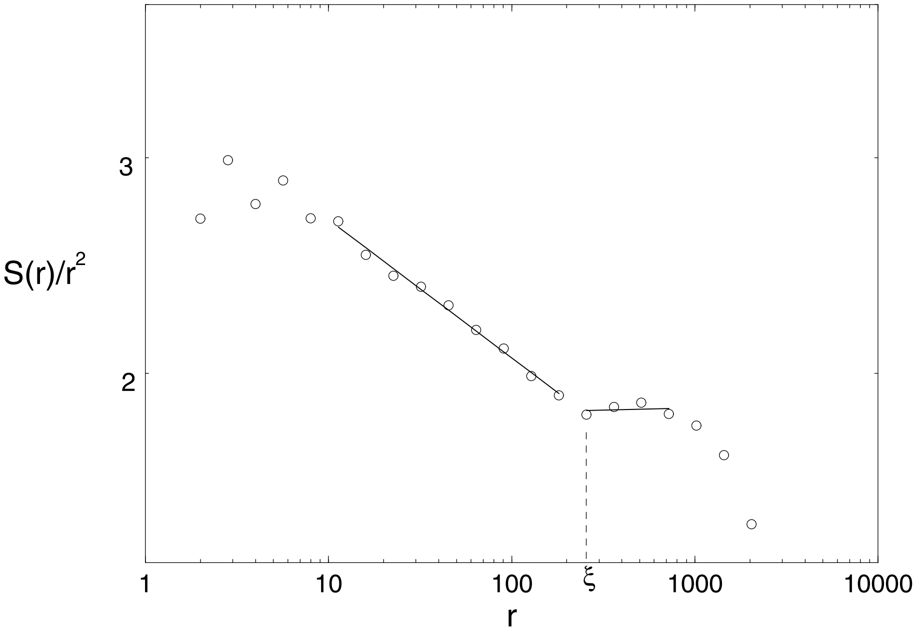

Fig. 2.7. The structure of the infinite percolation cluster above p_c. The dependence of the fractal dimension upon the length scale (Eq. (2.5)) is clearly seen in this plot of $S(r)/r^d$ ($d = 2$) versus r, for the infinite cluster in a 2500 × 2500 percolation system. The slope of the curve is $d_f - d$ for $r < \xi \approx 200$, and zero for $r > \xi$.

invariant (or homogeneous). The situation is cartooned in Fig. 2.6, in which the infinite cluster above criticality is likened to a regular lattice of Sierpinski gaskets of size ξ each. The peculiar structure of the infinite cluster implies that its mass scales differently at distances shorter and larger than ξ:

$$S(r) \sim \begin{cases} r^{d_f} & r < \xi, \\ r^d & r > \xi. \end{cases} \tag{2.5}$$

Fig. 2.7 illustrates this crossover measured in a two-dimensional percolation system above p_c.

We can now identify d_f by relating it to other critical exponents. An arbitrary site, within a given region of volume V, belongs to the infinite cluster with probability S/V (S is the mass of the infinite cluster enclosed within V). If the linear size of the region is smaller than ξ the cluster is self-similar, and so

$$P_\infty \sim \frac{r^{d_f}}{r^d} \sim \frac{\xi^{d_f}}{\xi^d}, \qquad r < \xi. \tag{2.6}$$

Using Eqs. (2.1) and (2.2) we can express both sides of Eq. (2.6) as powers of

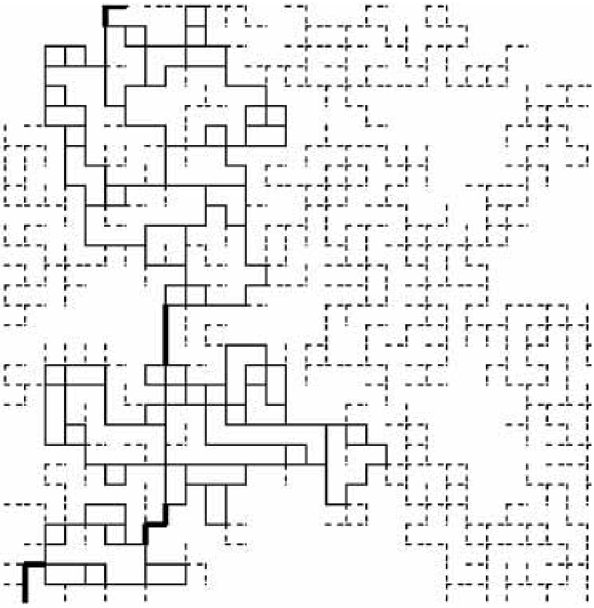

Fig. 2.8. Subsets of the incipient infinite percolation cluster. The spanning cluster (from top to bottom of the lattice) in a computer simulation of bond percolation on the square lattice at criticality is shown. Subsets of the cluster are highlighted: dangling ends (broken lines), blobs (solid lines), and red bonds (bold solid lines).

$p - p_{\mathrm{c}}$:

$$(p - p_{\mathrm{c}})^{\beta} \sim (p - p_{\mathrm{c}})^{-\nu(d_{\mathrm{f}}-d)}, \tag{2.7}$$

hence

$$d_{\mathrm{f}} = d - \frac{\beta}{\nu}. \tag{2.8}$$

Thus, the fractal dimension of percolation is not a new, independent exponent, but depends on the critical exponents β and ν. Since β and ν are universal, d_{f} is also universal!

2.3 Structural properties

As with other fractals, the fractal dimension is not sufficient to fully characterize the geometrical properties of percolation clusters. Different geometrical properties are important according to the physical application of the percolation model.

Suppose that one applies a voltage on two sites of a metallic percolation cluster. The *backbone* of the cluster consists of those bonds (or sites) which carry the electric current. The remaining parts of the cluster which carry no current are

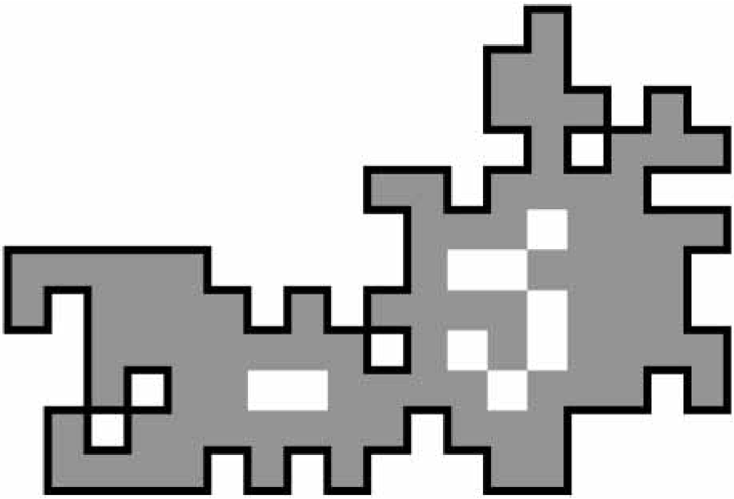

Fig. 2.9. The hull of percolation clusters. The external perimeter (the hull) is highlighted in bold lines in this computer simulation of a cluster of site percolation in the square lattice. The *total perimeter* includes also the edges of the internal "lakes" (not shown).

the *dangling ends* (Fig. 2.8). They are connected to the backbone by a single bond. The *red bonds* are those bonds that carry the total current; severing a red bond stops the current flow. The *blobs* are what remains from the backbone when all the red bonds are removed (Fig. 2.8). Percolation clusters (in the self-similar regime) are finitely ramified: arbitrarily large subsets of a cluster may always be isolated by cutting a finite number of red bonds.

The external perimeter of a cluster, which is also called the *hull*, consists of those cluster sites which are connected to infinity through an uninterrupted chain of empty sites (Fig. 2.9). In contrast, the *total perimeter* includes also the edges of internal holes. The hull is an important model for random fractal interfaces.

The fractal dimension of the backbone, $d_{\mathrm{f}}^{\mathrm{BB}}$, is smaller than the fractal dimension of the cluster (see Table 2.2). That is to say, most of the mass of the percolation cluster is concentrated in the dangling ends, and the fractal dimension of the dangling ends is equal to that of the infinite cluster. The fractal dimension of the backbone is known only from numerical simulations.

The fractal dimensions of the red bonds and of the hull are known from exact arguments. The mean number of red bonds has been shown to vary with p as $\langle N \rangle \sim (p - p_{\mathrm{c}})^{-1} \sim \xi^{1/\nu}$, hence the fractal dimension of red bonds is $d_{\mathrm{red}} = 1/\nu$. The fractal dimension of the hull in $d = 2$ is $d_{\mathrm{h}} = \frac{7}{4}$ – smaller than the fractal dimension of the cluster, $d_{\mathrm{f}} = 91/48$. In $d \geq 3$, however, the mass of the hull is believed to be proportional to the mass of the cluster, and both have the same fractal dimension.

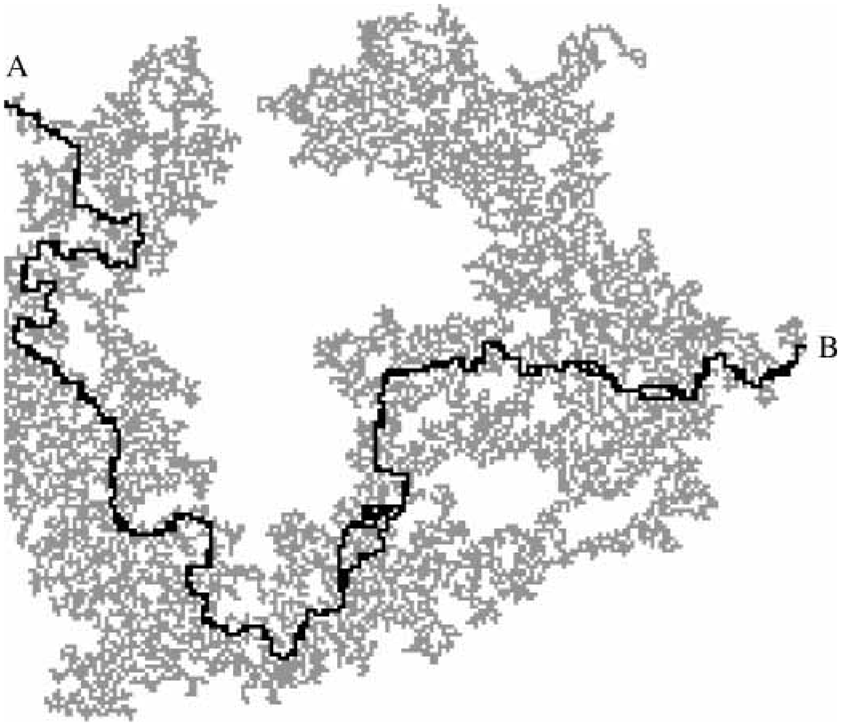

Fig. 2.10. Chemical distance. The chemical path between two sites A and B in a two-dimensional percolation cluster is shown in black. Notice that more than one chemical path may exist. The union of all the chemical paths shown is called the *elastic backbone*.

As an additional characterization of percolation clusters we mention the *chemical distance*. The chemical distance, ℓ, is the length of the shortest path (along cluster sites) between two sites of the cluster (Fig. 2.10). The *chemical dimension* d_ℓ, also known as the *graph dimension* or the *topological dimension*, describes how the mass of the cluster within a chemical length ℓ scales with ℓ:

$$S(\ell) \sim \ell^{d_\ell}. \tag{2.9}$$

By comparing Eqs. (2.4) and (2.9), one can infer the relation between regular Euclidean distance and chemical distance:

$$r \sim \ell^{d_\ell/d_\mathrm{f}} \equiv \ell^{\nu_\ell}. \tag{2.10}$$

This relation is often written as $\ell \sim r^{d_\mathrm{min}}$, where $d_\mathrm{min} \equiv 1/\nu_\ell$ can be regarded as the fractal dimension of the minimal path. The exponent d_min is known mainly from numerical simulations. Obviously, $d_\mathrm{min} \geq 1$ (see Table 2.2). In many known deterministic fractals the chemical length exponent is either $d_\ell = d_\mathrm{f}$ (e.g., for the Sierpinski gasket) or $d_\ell = 1$ (e.g., for the Koch curve). An example of an

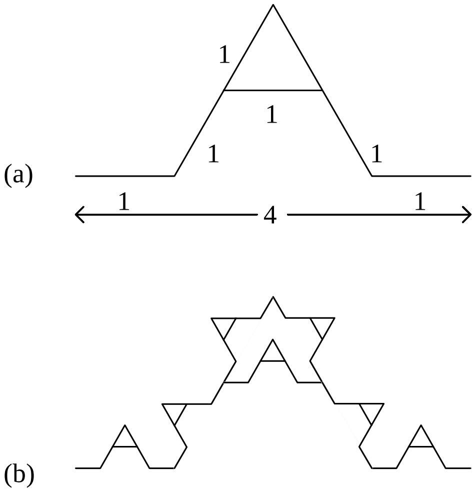

Fig. 2.11. The modified Koch curve. The initiator consists of a unit segment. Shown is the curve after one generation (a), and two generations (b). Notice that the shortest path (i.e., the chemical length) between the two endpoints in (a) is five units long.

exception to this rule is exhibited by the modified Koch curve of Fig. 2.11. The fractal dimension of this object is $d_{\mathrm{f}} = \ln 7/\ln 4$, while its chemical dimension is $d_\ell = \ln 7/\ln 5$ (or $d_{\mathrm{min}} = \ln 5/\ln 4$).

The concept of chemical length finds several interesting applications, such as in the *Leath algorithm* for the construction of percolation clusters (Exercise 2), or in oil recovery, in which the first-passage time from the injection well to a production well a distance r away is related to ℓ. It is also useful in the description of propagation of epidemics and forest fires. Suppose that trees in a forest are distributed as in the percolation model. Assume further that in a forest fire at each unit time a burning tree ignites fires in the trees immediately adjacent to it (the nearest neighbors). The fire front will then advance one *chemical shell* (sites at equal chemical distance from a common origin) per unit time. The speed of propagation would be

$$v = \frac{dr}{dt} = \frac{dr}{d\ell} \sim \ell^{\nu_\ell - 1} \sim (p - p_{\mathrm{c}})^{\nu(d_{\mathrm{min}} - 1)}. \tag{2.11}$$

In $d = 2$ the exponent $\nu(d_{\mathrm{min}} - 1) \approx 0.16$ is rather small and so the increase of v upon crossing p_{c} is steep: a fire that could not propagate at all below p_{c} may propagate very fast just above p_{c}, when the concentration of trees is only slightly bigger.

In Table 2.2 we list the values of some of the percolation exponents discussed above. As mentioned earlier, they are universal and depend only on the dimension-

Table 2.2. *Fractal dimensions of the substructures composing percolation clusters.*

d	2	3	4	5	6
d_f	$91/48$[a]	2.53 ± 0.02[b]	3.05 ± 0.05[c]	3.69 ± 0.02[d]	4
d_min	1.1307 ± 0.0004[e]	1.374 ± 0.004[e]	1.60 ± 0.05[f]	1.799[g]	2
d_red	$3/4$[h]	1.143 ± 0.01[i]	1.385 ± 0.055[j]	1.75 ± 0.01[j]	2
d_h	$7/4$[k]	2.548 ± 0.014[i]			4
d_f^BB	1.6432 ± 0.0008[l]	1.87 ± 0.03[m]	1.9 ± 0.2[n]	1.93 ± 0.16[n]	2
ν	$4/3$[a]	0.88 ± 0.02[c]	0.689 ± 0.010[p]	0.571 ± 0.003[q]	1/2
τ	$187/91$[r]	2.186 ± 0.002[b]	2.31 ± 0.02[r]	2.355 ± 0.007[r]	5/2

[a] den Nijs (1979), Nienhuis (1982); [b] Jan and Stauffer (1998). Other simulations (Lorenz and Ziff, 1998) yield $\tau = 2.189 \pm 0.002$; [c] Grassberger (1983; 1986); [d] Jan *et al.* (1985); [e] Grassberger (1992a). Earlier simulations (Herrmann and Stanley, 1988) yield $d_\mathrm{min} = 1.130 \pm 0.004$ ($d = 2$); [f] calculated from $d_\mathrm{min} = 1/\nu_\ell$; [g] Janssen (1985), from ϵ-expansions; [h] Coniglio (1981; 1982); [i] Strenski *et al.* (1991); [j] calculated from $d_\mathrm{red} = 1/\nu$; [k] Sapoval *et al.* (1985), Saleur and Duplantier (1987); [l] Grassberger (1999a); [m] Porto *et al.* (1997b). Series expansions (Bhatti *et al.*, 1997) yield $d_\mathrm{f}^\mathrm{BB} = 1.605 \pm 0.015$; [n] Hong and Stanley (1983a); [p] Ballesteros *et al.* (1997). They also find $\eta = 2 - \gamma/2 = 0.0944 \pm 0.0017$; [q] Adler *et al.* (1990); and [r] calculated from $\tau = 1 + d/d_\mathrm{f}$. For the meaning of τ, see Section 2.4. Notice also that β and γ may be obtained from the other exponents, for example: $\beta = \nu(d - d_\mathrm{f})$, $\gamma = \beta(\tau - 2)/(3 - \tau)$.

ality of space, not on other details of the percolation model. Above $d = 6$ loops in the percolation clusters are too rare to play any significant role and they can be neglected. Consequently, the values of the critical exponents for $d > 6$ are exactly the same as for $d = 6$. The dimension $d = d_\mathrm{c} = 6$ is called the *upper critical dimension*. The exponents for $d \geq d_\mathrm{c}$ may be computed exactly, as we show in the next section.

2.4 Percolation on the Cayley tree and scaling

The Cayley tree is a loopless lattice, generated as follows. From a central site – the *root*, or *origin* – there emanate z branches. The end of each branch is a site, so there are z sites, which constitute the first shell of the Cayley tree. From each site of the first (chemical) shell there emanate $z - 1$ branches, generating $z(z - 1)$ sites, which constitute the second shell. In the same fashion, from each site of the ℓth shell there emanate $z - 1$ new branches whose endpoints are sites of the $(\ell + 1)$th shell (Fig. 2.12). The ℓth shell contains $z(z - 1)^{\ell-1}$ sites and therefore the Cayley tree may be regarded as a lattice of infinite dimension, since the number of sites grows exponentially – faster than any power law. The absence of loops in the

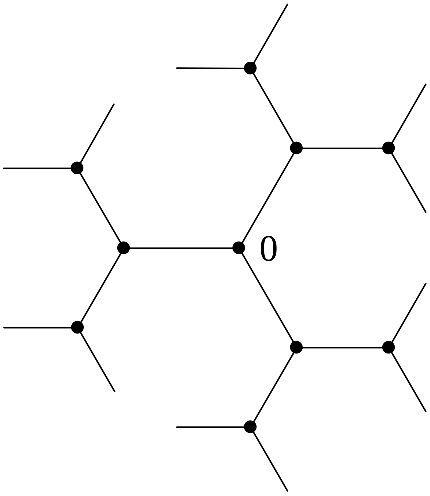

Fig. 2.12. The Cayley tree with $z = 3$. The chemical shells $\ell = 0$ (the “origin”, 0), $\ell = 1$, and $\ell = 2$ are shown.

Cayley tree allows one to solve the percolation model (and other physics models) exactly. We now demonstrate how to obtain the percolation exponents for $d \geq 6$.

We must address the issue of distances beforehand. The Cayley tree cannot be embedded in any lattice of finite dimension, and so instead of Euclidean distance one must work with chemical distance. Because of the lack of loops there is only one path between any two sites, whose length is then by definition the chemical length ℓ. Above the critical dimension $d \geq d_{\mathrm{c}} = 6$ we expect that correlations are negligible and that any path on a percolation cluster is essentially a random walk; $r^2 \sim \ell$, or

$$d_{\mathrm{min}} = 2, \tag{2.12}$$

(cf. Eq. (2.10)). This connects Euclidean distance to chemical distance.

Consider now a percolation cluster on the Cayley tree. Suppose that the origin is part of a cluster. In the first shell, there are on average $\langle s_1 \rangle = pz$ sites belonging to that same cluster. The average number of cluster sites in the $(\ell + 1)$th shell is $\langle s_{\ell+1} \rangle = \langle s_\ell \rangle p(z - 1)$. Thus,

$$\langle s_\ell \rangle = z(z - 1)^{\ell-1} p^\ell = zp[(z - 1)p]^{\ell-1}. \tag{2.13}$$

From this we can deduce p_{c}: when $\ell \to \infty$ the number of sites in the ℓth shell tends to zero if $p(z - 1) < 1$, whereas it diverges if $p(z - 1) > 1$; hence

$$p_{\mathrm{c}} = \frac{1}{z - 1}. \tag{2.14}$$

For $p < p_{\mathrm{c}}$, the density of cluster sites in the ℓth shell is $\langle s_\ell \rangle / \sum_{\ell=1}^{\infty} \langle s_\ell \rangle$.

Therefore the correlation length in chemical distance is (using Eqs. (2.13) and (2.14))

$$\xi_\ell = \frac{\sum_{\ell=1}^{\infty} \ell \langle s_\ell \rangle}{\sum_{\ell=1}^{\infty} \langle s_\ell \rangle} = \frac{p_c}{p_c - p}, \qquad p < p_c. \tag{2.15}$$

The correlation length in regular space is $\xi \sim \xi_\ell^{\nu_\ell}$, and therefore

$$\xi \sim (p_c - p)^{-1/2}, \tag{2.16}$$

or $\nu = \frac{1}{2}$. The mean mass of the finite clusters (below p_c) is

$$S = 1 + \sum_{\ell=1}^{\infty} \langle s_\ell \rangle = p_c \frac{1+p}{p_c - p} = (p_c - p)^{-\gamma}, \tag{2.17}$$

which yields $\gamma = 1$ for percolation on the Cayley tree.

Consider next sn_s, the probability that a given site belongs to a cluster of s sites. The quantity n_s is the analogous probability *per cluster site*, or the probability distribution of cluster sizes in a percolation system. Suppose that a cluster of s sites possesses t perimeter sites (empty sites adjacent to the cluster). The probability of such a configuration is $p^s(1-p)^t$. Hence,

$$n_s = \sum_t g_{s,t} p^s (1-p)^t, \tag{2.18}$$

where $g_{s,t}$ is the number of possible configurations of s-clusters with t perimeter sites. In the Cayley tree all s-site clusters have exactly $2 + (z-2)s$ perimeter sites, and Eq. (2.18) reduces to

$$n_s(p) = g_s p^s (1-p)^{2+(z-2)s}, \tag{2.19}$$

where now g_s is simply the number of possible configurations of an s-cluster. We are interested in the behavior of n_s near the percolation transition. Expanding Eq. (2.19) around $p_c = 1/(z-1)$ to lowest order in $p - p_c$ yields

$$n_s(p) \sim n_s(p_c) \exp[-(p - p_c)^2 s]. \tag{2.20}$$

To estimate $n_s(p_c)$ we need to compute g_s, which can be done through exact combinatorics arguments. The end result is that n_s behaves as a power law, $n_s(p_c) \sim s^{-\tau}$, with $\tau = \frac{5}{2}$. The above behavior of n_s is also typical of percolation in $d < 6$ dimensions. Generally,

$$n_s \sim s^{-\tau} f((p - p_c)s^\sigma), \tag{2.21}$$

where $f(x)$ is a *scaling function* that decays rapidly for large $|x|$. Thus n_s decays as $s^{-\tau}$ until some cutoff size $s_* \sim |p - p_c|^{1/\sigma}$, whereupon it quickly drops to zero. For percolation in the Cayley tree $f(x)$ is the exponential in Eq. (2.20), and so $\sigma = \frac{1}{2}$.

We will now use the scaling form of n_s to compute τ in yet another way. To this end we re-compute the mean mass of finite clusters, S, in terms of n_s. Since sn_s is the probability that an arbitrary site belongs to an s-cluster, $\sum sn_s = p\ (p < p_\mathrm{c})$. The mean mass of finite clusters is

$$S = \frac{\sum_s^\infty s\, sn_s}{\sum_s^\infty sn_s} \sim \frac{1}{p}\sum_s^{s_*} s^2 n_s \sim (p_\mathrm{c} - p)^{-(3-\tau)/\sigma}, \tag{2.22}$$

where we have used the scaling of n_s (and of the cutoff at s_*), and we assume that $\tau < 3$. By comparing this to Eq. (2.17) one obtains the scaling relation

$$\gamma = \frac{3-\tau}{\sigma}. \tag{2.23}$$

For percolation in the Cayley tree we see that $\tau = \frac{5}{2}$ (consistent with the assumption that $\tau < 3$).

Finally, let us compute the order-parameter exponent β. Any site in the percolation system is (a) empty, with probability $1 - p$, (b) occupied and on the infinite cluster, with probability pP_∞, or (c) occupied but not on the infinite cluster, with probability $p(1 - P_\infty)$. Therefore,

$$P_\infty = 1 - \frac{1}{p}\sum_s sn_s. \tag{2.24}$$

For $p < p_\mathrm{c}$ all clusters are finite, $\sum sn_s = p$, and $P_\infty = 0$. Above criticality $\sum sn_s$ is smaller than p, because there are occupied sites that belong to the infinite cluster. The correction comes from the upper cutoff of the sum at $s = s_*$; $\sum sn_s \sim \sum^{s_*} s^{1-\tau} \sim p - [\text{constant} \times (p - p_\mathrm{c})^{-(2-\tau)/\sigma}]$. We then find the scaling relation

$$\beta = \frac{\tau - 2}{\sigma}, \tag{2.25}$$

and so $\beta = 1$ for percolation on the Cayley tree and for percolation in $d \geq 6$.

In closing this chapter, we would like to mention that there exist several variations of the percolation model that lie in different universality classes than regular percolation. These include directed percolation, invasion percolation, and long-range correlated percolation.

2.5 Exercises

1. Simulate percolation on the computer, following the simple-minded method of Section 2.1. Devise an algorithm to find out whether there is a spanning percolation cluster between any two sites, and to identify all the sites of the incipient percolation cluster.

2. *The Leath algorithm.* Percolation clusters can be built one chemical shell at a time, by using the Leath algorithm. Starting with an origin site (which represents the chemical shell $\ell = 0$) its nearest neighbors are assigned to the first chemical shell with probability p. The sites which were not chosen are simply marked as having been "inspected". Generally, given the first ℓ shells of a cluster, the $(\ell + 1)$th shell is constructed as follows: identify the set of nearest neighbors to the sites of shell ℓ. From this set discard any sites that belong to the cluster, or which are already marked as "inspected". The remaining sites belong to shell $(\ell + 1)$ with probability p. Remember to mark the newly inspected sites which were left out. Simulate percolation clusters at p slightly larger than p_{c} and confirm the crossover of Eq. (2.5).
3. Imagine an *anisotropic* percolation system in $d = 2$ with long range correlations, such that the correlation length depends on direction:

$$\xi_x \sim (p - p_{\mathrm{c}})^{-\nu_x}, \qquad \xi_y \sim (p - p_{\mathrm{c}})^{-\nu_y}.$$

   Generalize the formula $d_{\mathrm{f}} = d - \beta/\nu$ for this case. (Answer: $d_{\mathrm{f}}^x = 1 + (\nu_y - \beta)/\nu_x$; $d_{\mathrm{f}}^y = 1 + (\nu_x - \beta)/\nu_y$.)
4. From our presentation of the Cayley tree it would seem that the root of the tree is a special point. Show, to the contrary, that in an infinite Cayley tree all sites are equivalent!
5. Show that, in the Cayley tree, an s-cluster has exactly $2 + (z - 2)s$ perimeter sites. (Hint: prove it by induction.)
6. The exponent α is defined by the relation $\sum_s n_s \sim |p - p_{\mathrm{c}}|^{2-\alpha}$. In thermodynamic phase transitions, α characterizes the divergence of the *specific heat*. Show that $2 - \alpha = (\tau - 1)/\sigma$.
7. The critical exponent δ characterizes the response to an external ordering field h. For percolation, it may be defined as $\sum_s s\, n_s e^{-hs} \sim h^{1/\delta}$. Show that $\delta = 1/(\tau - 2)$.
8. The exponents α, β, γ, and δ can all be written in terms of σ and τ. Therefore, any two exponents suffice to express the others. As an example, express α, δ, σ, and τ as functions of β and γ.
9. Percolation in one dimension may be analyzed exactly. Notice that only the subcritical phase exists, since $p_{\mathrm{c}} = 1$. Analyze this problem directly and compare it with the limit of percolation in the Cayley tree when $z \to 2$.
10. Define the largest cluster in a percolation system as having rank $\rho = 1$, the second largest $\rho = 2$, and so on. Show that, at criticality, the mass of the clusters scales with rank as $s \sim \rho^{-d/d_{\mathrm{f}}}$.

2.6 Open challenges

Percolation is the subject of much ongoing research. There remain many difficult theoretical open questions, such as finding exact percolation thresholds, and the exact values of various critical exponents. Until these problems are resolved, there is a point in improving the accepted numerical values of such parameters through simulations and other numerical techniques. Often this can be achieved using well-worn approaches, simply because computers get better with time! Here is a sample of interesting open problems.

1. The critical exponents β and ν are known exactly for $d = 2$, due to the relation of percolation to the one-state Potts model. However, no exact values exist for β and ν in $2 < d < 6$, nor for d_f^BB and d_min in all $1 < d < 6$. Also, is d_h truly equal to d_f in three-dimensional percolation, as is commonly assumed?
2. Series expansions (Bhatti *et al.*, 1997) suggest that d_min is nonuniversal: for the square lattice $d_\mathrm{min} = 1.106 \pm 0.007$, whereas for the triangular lattice $d_\mathrm{min} = 1.148 \pm 0.007$. Extensive numerical analysis is needed to clinch this issue. Numerical estimates for critical exponents in continuum percolation are currently markedly different than the universal values on lattices (Okazaki *et al.*, 1996; Balberg, 1998a; Rubin *et al.*, 1999). Simulations of larger systems, and closer to the transition point, are necessary to probe this issue.
3. Most values of the critical percolation thresholds are not known exactly. There is an ongoing search for expressions containing the various p_c which might be universal (Galam and Mauger, 1997; 1998; Babalievski, 1997; van der Marck, 1998).
4. Improve existing numerical algorithms for percolation, or invent new fresh ones. Researchers in the area keep finding better ways to perform the same old tricks! An example of this trend is the recent introduction of a new efficient algorithm for the identification of percolation backbones (Moukarzel, 1998). See also Babalievski (1998) and Stoll (1998).
5. Little is known about anisotropic percolation (see, for example, Dayan *et al.* (1991)). Transport properties of such models have not been studied.
6. It was commonly believed until recently that, for percolation in two-dimensional lattices at p_c, there exists exactly one incipient spanning cluster. New insight into this question was achieved by Aizenman (1997) when he proved that the number of incipient spanning clusters can be larger than one, and the probability of having at least k separate clusters in a system of size $L \times L$, $P_L(k)$, is bounded by $Ae^{-\alpha k^2} \leq P_L(k) \leq Ae^{-\alpha' k^2}$, where α and α' are constants. Numerical estimates for A, α, and α' were given by Shchur and Kosyakov (1998).
7. Percolation with long-range correlations has been studied by Prakash *et al.*

(1992), Makse *et al.* (1996), and Moukarzel *et al.* (1997). Makse *et al.* (1995) have applied the model to the study of the structure of cities. There remain many open questions.

8. The traditional percolation model assumes that one has only one kind of sites or bonds. Suppose for example that the bonds are of two different kinds: ε_1 and ε_2. One may then search for the path between two given points on which the sum of ε_i is minimal. This is the optimal-path problem (Cieplak *et al.*, 1994; 1996; Schwartz *et al.*, 1998). The relation of this problem to percolation is still open for research.
9. Are there other universal properties of percolation, in addition to the critical exponents and amplitude ratios? For example, results of recent studies by Cardy (1998), Aizenman (1997), and Langlands (1994) suggest that the crossing probability $\pi(\Omega)$ is a universal function of the shape of the boundary Ω of the percolation system.
10. Is there self-averaging in percolation, i.e., can ensemble averages be replaced by an average over one large (infinite) cluster? See De Martino and Giansanti (1998a; 1998b).

2.7 Further reading

- Reference books on percolation: Stauffer and Aharony (1994), and Bunde and Havlin (1996; 1999). For applications, see Sahimi (1994). A mathematical approach is presented by Essam (1980), Kesten (1982), and Grimmet (1989).
- Numerical methods for the generation of the backbone: Herrmann *et al.* (1984b), Porto *et al.* (1997b), Moukarzel (1998), and Grassberger (1999a). Experimental studies of the backbone in epoxy-resin–polypyrrol composites using image-analysis techniques can be found in Fournier *et al.* (1997).
- The fractal dimension of the red bonds: Coniglio (1981; 1982). Red bonds on the “elastic” backbone: Sen (1997). The fractal dimension of the hull: Sapoval *et al.* (1985) and Saleur and Duplantier (1987).
- Exact results for the number of clusters per site for percolation in two dimensions were presented by Kleban and Ziff (1998).
- Series-expansion analyses: Adler (1984). The renormalization-group approach: Reynolds *et al.* (1980). A renormalization-group analysis of several quantities such as the minimal path, longest path, and backbone mass has been presented by Hovi and Aharony (1997a). A recent renormalization-group analysis of the fractal dimension of the backbone, d_f^BB, to third-order in $\epsilon = 6 - d$ is given by Janssen *et al.* (1999).
- Forest fires in percolation: see, for example, Bak *et al.* (1990), Drossel and Schwabl (1992), and Clar *et al.* (1997).

- Continuum percolation: Balberg (1987). Experimental studies of continuum percolation in graphite–boron nitrides: Wu and McLachlan (1997). A recent study of percolation of finite-sized objects with applications to the transport properties of impurity-doped oxide perovskites: Amritkar and Roy (1998). Invasion percolation: Wilkinson and Willemsen (1983), Porto *et al.* (1997a), and Schwarzer *et al.* (1999). Directed percolation: Kinzel (1983), Frojdh and den Nijs (1997), and Cardy and Colaiori (1999).
- Percolation on fractal carpets: Havlin *et al.* (1983a) and Lin *et al.* (1997).
- A problem related to percolation that includes also long-range bonds, the "small-world network", has been studied by Watts and Strogatz (1998). They find that adding a very small fraction of randomly connected long-range bonds reduces the chemical distance dramatically. For interesting applications of the "small-world network" see Lubkin (1998).
- A new approach based on generating functions for percolation in the Cayley tree can be found in Buldyrev *et al.* (1995a).
- Applications of percolation theory and chemical distance to recovery of oil from porous media: Dokholyan *et al.* (1999), King *et al.* (1999), Lee *et al.* (1999), and Porto *et al.* (1999). Applications to ionic transport in glasses and composites: Roman *et al.* (1986), Bunde *et al.* (1994), and Meyer *et al.* (1996a). Applications to the metal–insulator transition: see, for example, Ball *et al.* (1994). Applications to fragmentation: see, for example, Herrmann and Roux (1990), Sokolov and Blumen (1999), and Cheon *et al.* (1999).